Proceedings of the ASME 2018
Pressure Vessels and Piping Conference
PVP2018
July 15-20, 2018, Prague, Czech Republic

PVP2018-84910

CASE STUDIES ON THE USE OF THERMAL-MECHANICAL FINITE ELEMENT ANALYSIS TO EVALUATE WELD RING GASKET AND DIAPHRAGM SEAL DESIGNS

Phillip E. Prueter, P.E.

Robert C. Davis, P.E.

Clay D. Rodery

Stephen F. McJones

Richard P. Brodzinski

Josh Havekost

Daniel E. Feddeler

ABSTRACT

Weld ring type gaskets are relatively common in the refining and petrochemical industries. These gasket configurations usually consist of two steel rings, fillet-welded to each of the mating flanges with another seal weld between the lips of the two rings. These seal welds or lip seals are sometimes prone to in-service cracking that can eventually lead to leakage and costly equipment downtime. One particular design feature that can significantly influence the propensity for leakage is the shape of the weld rings; flat-lip weld rings or hollow-lip (Omega-seal) weld rings are the two most commonly used designs. The hollow-lip designs inherently offer more flexibility and can generally accommodate more differential radial thermal expansion between mating flanges.

This paper highlights a case study of a high-pressure heat exchanger where the shell side-to-tube side girth flange joint is fitted with a weld ring gasket configuration. Comparisons are made using detailed finite element analysis (FEA) that include bolt pretension and pressure-temperature loading. Sensitivity to lip seal design, temperature profile, and assumed friction coefficient between seating surfaces is also investigated. Furthermore, general commentary on flat and hollow lip weld ring gasket geometries is provided with design recommendations for different applications. In summary, the flat-lip seal weld experiences high shear stress, even with small amounts of differential temperature between flanges, which makes it prone to cracking. The added compliance of the hollow-lip seal design can minimize stresses in the seal weld, but understanding operating temperature differen-

tials between mating flanges represents a key aspect of ensuring leak-free operation. The design of a diaphragm seal on a flat heat exchanger channel cover is also evaluated using FEA techniques, with sensitivity analysis on the size of the external fillet weld and diaphragm material specification. The analysis techniques presented in this paper offer valuable insight into establishing damage tolerant weld ring gasket and diaphragm seal designs to minimize the potential for leakage and to optimize critical gasket and bolting parameters.

INTRODUCTION

Weld ring gasket configurations are typically used in critical applications where leakage is not tolerable (combustible or hazardous process fluid). Figure 1 shows sketches of flat-lip seal and a hollow-lip (Omega) seal welded gasket designs (note that the schematics in this figure come from Reference [1]). Commonly, weld ring gasket designs involve the mating of two separate weld rings, where each ring is welded to its respective flange via an attachment fillet weld, and then following assembly, the outer edge of the two rings are welded together at the seal weld seam location. Figure 1 points out the seal and attachment fillet welds on both the flat and hollow-lip seal configurations. It is noted that depending on the specific weld ring gasket design, the attachment fillet welds can either be on the inside or outside diameter of the rings.

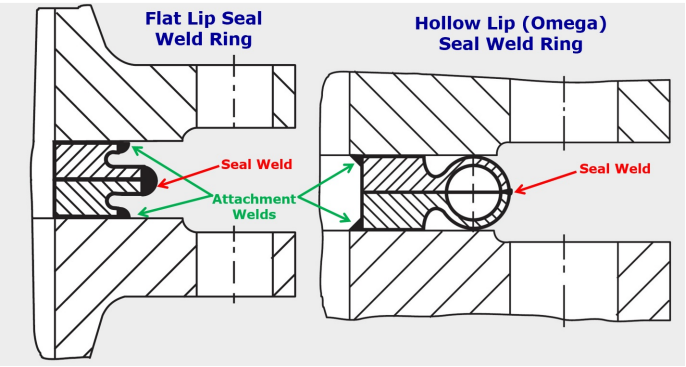

Figure 1. Sketches of Flat and Hollow-Lip (Omega) Seal Weld Ring Gasket Designs.

This paper outlines a computational study that was performed following a failure (leak) in a bolted joint on an in-service high-pressure heat exchanger. The leak resulted from a through-thickness crack in the seal weld on flat-lip weld ring gaskets that were intended to seal the interface of the channel (tube-side) flange, with an integral tubesheet, and the shell-side flange. Figure 2 shows a sketch of the specific heat exchanger weld ring gasket configuration that leaked in-service. This configuration consists of attachment welds to the flange faces on the inside diameter of the rings, as shown.

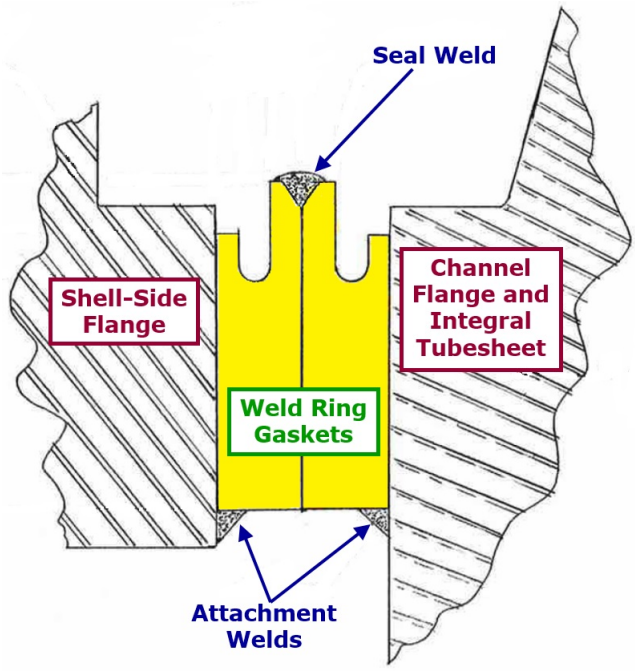

Figure 2. Sketch of the Flat-Lip Seal Weld Ring Gasket Configuration that Leaked In-Service.

Following a thermal-mechanical FEA-based root cause failure investigation of the weld ring gasket design shown in Figure 2, additional analysis was performed on alternative lip seal designs, including a hollow-lip (Omega) design. These analyses are summarized herein and include evaluation of stresses in the gasket attachment and seal welds, as well as overall sealing capability (compressive stresses and deflections under bolt loading, pressure, and steady-state operating temperatures). Additionally, comparisons of different diaphragm seal designs on the flat head (cover) of the same heat exchanger channel are outlined in this paper. The original diaphragm seal configuration investigated is shown in Figure 3. This analysis investigates the behavior of the channel cover diaphragm seal, including stresses in the fillet weld and overall gasket compression characteristics.

A simplified general layout drawing of the heat exchanger in question is shown in Figure 4 (with the locations of the weld ring gasket and diaphragm seal in question identified). This horizontal exchanger has a U-tube bundle layout, and the prospect of a leak in-service carries a relatively high consequence of failure. As discussed in Reference [2], in a U-tube heat exchanger, the effect of axial thermal expansion or contraction of the shell relative to the tube bundle (due to differential metal temperatures) is decoupled. Additionally, this heat exchanger is characterized

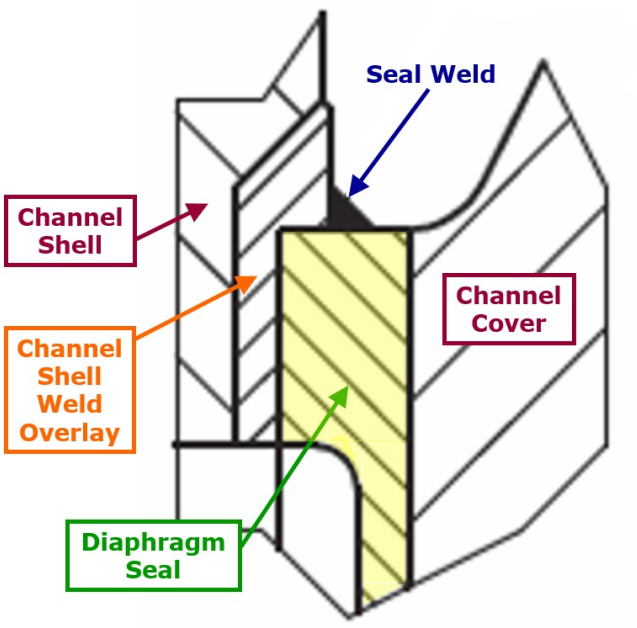

Figure 3. Original Channel Cover Diaphragm Seal Configuration with Seal Weld.

as a Type CEU design in accordance with the Tubular Exchanger Manufacturers Association (see Reference [3]), indicating it has a channel with an integral tubesheet, a one-pass shell, and a U-tube bundle. Furthermore, the approximate design conditions of the heat exchanger are as follows:

- Year of Construction: 2010
- Design Code: ASME Section VIII Division 1 [4]
- Shell-Side Design Pressure: 2,400 psi
- Shell-Side Design Temperature: 650°F
- Tube-Side Design Pressure: 2,200 psi
- Tube-Side Design Temperature: 800°F
- Shell-Side/Tube-Side Inside Diameter: 50 inches
- Shell-Side/Tube-Side Base Metal: 2-1/4-Cr-1-Mo
- Shell-Side/Tube-Side Weld Overlay: Stainless Steel

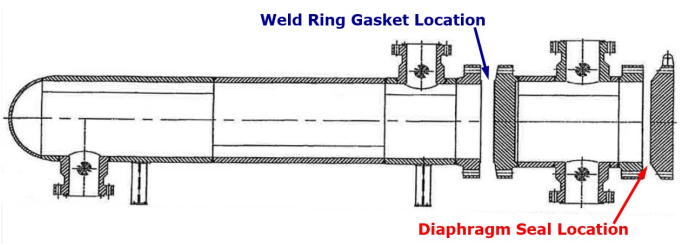

Figure 4. Simplified General Layout Drawing of Heat Exchanger Evaluated Herein.

LITERATURE REVIEW

Numerous technical investigations have been published that focus on assessing the gasket design and sealing capability of bolted (flanged) joints. In the oil refining, chemical, and power generation industries, this topic is particularly relevant for heat exchanger, pressure vessel, and piping component bolted connections with gasket or diaphragm seals. Reference [5] summarizes the successful removal of a high-pressure heat exchanger (in the refining industry) tube-side cover plate diaphragm and subsequent replacement with a metal pressure-energized seal ring. Furthermore, this modification reportedly resulted in a 75 percent savings in reassembly costs, and led to a more reliable and leak free bolted joint. Additionally, detailed computational analysis of a diaphragm closure by McGuffie et al. [6] employed thermal-mechanical FEA to quantify operating temperature differentials and overall joint integrity.

In 1994, Martens and Porter [7] published a FEA-based study that explored the thermal-mechanical behavior of a heat exchanger bolted joint that developed a leak in service. This analysis resulted in successful repair of the leaking joint using a weld ring gasket configuration. A follow-up evaluation on this same bolted joint was conducted in 2006 [8], where more advanced transient analysis was performed (enabled by advances in computing power relative to the study published 12 years earlier). Additionally, Sato and Kado [9] performed elastic-plastic FEA to evaluate the behavior of dissimilar material flanges with metal ring gaskets at elevated temperatures. A computational study performed by Prueter et al. [10] utilized three-dimensional (3D), non-linear FEA to evaluate the propensity for leakage in a multi-pass, floating head heat exchanger subject to operating temperature differentials (where the gasket, flanges, tubesheet, head, and bolts were directly modeled). This study also established simplified, yet accurate methods for estimating the stiffness of heat exchanger tube bundles in complex 3D FEA models.

Additional studies have addressed the topic of flanged joint behavior due to thermal-mechanical loading. Early work by Dudley [11] and Kerkhof [12] examined an analytical approach to calculate stresses in flanges due to differential temperatures and the relaxation in bolt loads due to increased temperatures, respectively. Reference [13] summarizes the evaluation of a heat exchanger flange at elevated temperature. Additionally, several recent studies have investigated techniques to assess flanged joint behavior due to thermal loading. Brown and Brodzinski [14] employed analytical and finite element methods to assess the behavior of a flanged joint in a heat exchanger subjected to thermal and mechanical loading, where the effects of differential axial and radial thermal expansion at the joint were considered. Bouzid and Nechache presented a theoretical approach for determining steady-state operating temperatures and deflections in bolted joints and discussed an analytical method for evaluating variation in gasket stress due to internal fluid temperature in References [15] and [16], respectively. Also, Nagata and Sawa (see Reference [17]) utilized thermal-mechanical FEA to determine

the influence of temperature change on bolt and gasket load in ring type joint connections. A notable example of investigating potential leakage at a bolted joint in a heat exchanger under extreme operating (upset) conditions using a detailed FEA model is discussed in Reference [18]. Other FEA-based studies of flanged joints subjected to thermal-mechanical loading are reflected in References [19–26].

Other work by Brown et al. [27, 28] discusses the development of analytical techniques to evaluate steady-state temperatures and corresponding thermal expansion in flanged joints. Additionally, References [29–31] investigate gasket behavior due to differential thermal expansion and bolt relaxation. Validation of these approaches is performed by comparing results to FEA and experimental data. A thorough literature review relating to thermal loading in flanged joints as well as the development of a comprehensive method to evaluate the effects of temperature in flanged joints is discussed in WRC Bulletin 510 [32]. Lastly, a recent FEA-based study on the relaxation behavior of gaskets in typical flange connections is offered in Reference [33].

FINITE ELEMENT MODELS

In this study, axisymmetric FEA models are utilized to approximate the flanged joints in question, and appropriate assumptions regarding the treatment of the bolts and tubesheet are employed. Figure 5 shows the overall axisymmetric FEA model of the channel-to-shell-side flanged joint with the original (flat-lip) weld ring gaskets.

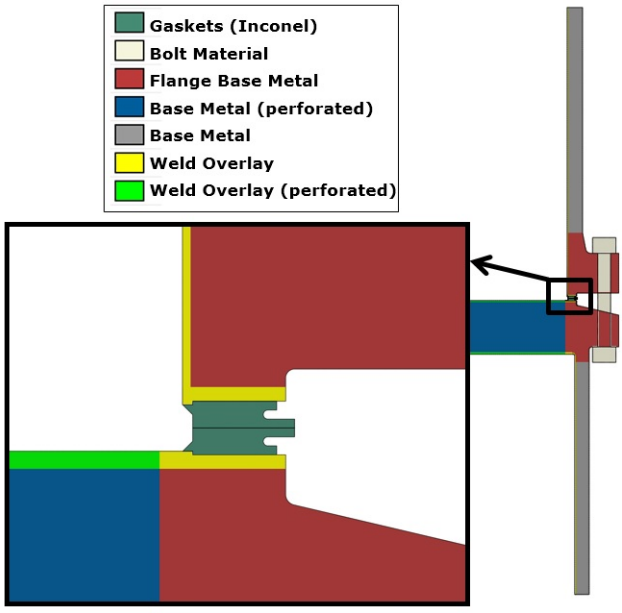

Figure 5. Axisymmetric FEA Model of the Channel-to-Shell-Side Flanged Joint with the Original (Flat-Lip) Weld Ring Gaskets.

The shell-side and tube-side base metal is 2-1/4-Cr-1-Mo with stainless steel weld overlay, and the weld ring gaskets are Inconel. In this model, orthotropic material properties are defined to mimic the presence of the holes in the perforated regions of the tubesheet. The tubesheet flange extension is tapered as shown in Figure 5. Additionally, equivalent plane stress elements are defined for the bolt cross-section to facilitate application of the total bolt load, and contact is defined between the weld ring gaskets and their respective flanges, as well as at the interface between the two mating gaskets. Furthermore, the gasket attachment and seal welds are idealized and simulated as being integrally connected (accomplished using tied surfaces). This is evident in Figure 6, which offers a close-up view of the gasket region on the FEA model with mesh refinement shown, and in Figure 7, which shows the contact and tied surfaces at the weld ring gasket assembly location.

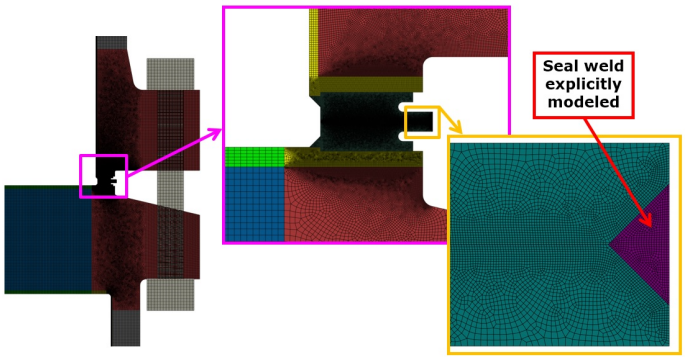

Figure 6. Mesh Refinement of the Channel-to-Shell-Side Flanged Joint with the Original (Flat-Lip) Weld Ring Gaskets.

An alternative weld ring gasket design for the same flanged joint that was evaluated using FEA is shown in Figure 8. This figure shows contact and tied surfaces at the weld ring gasket assembly location. This design incorporates a hollow-lip (Omega seal) weld ring gasket design, as shown. This modified design is investigated herein as a potential replacement to the original flat-lip seal configuration because hollow-lip weld ring gasket designs inherently offer more flexibility and can generally accommodate more differential movement or radial thermal expansion between mating flanges (thus, improving the damage tolerance of the seal weld and reducing the risk for cracking). Contrarily, flat-lip gasket designs can generally accommodate little-to-no differential radial movement between flanges. In fact, Reference [1] indicates that flat-lip designs are not recommended if differential radial expansion between gaskets exceeds 0.1 mm. Additionally, in the FEA (as shown in Figure 8), the attachment welds are tied to their respective flange faces, and the seal weld is tied together to mimic the joining of the hollow gasket lips.

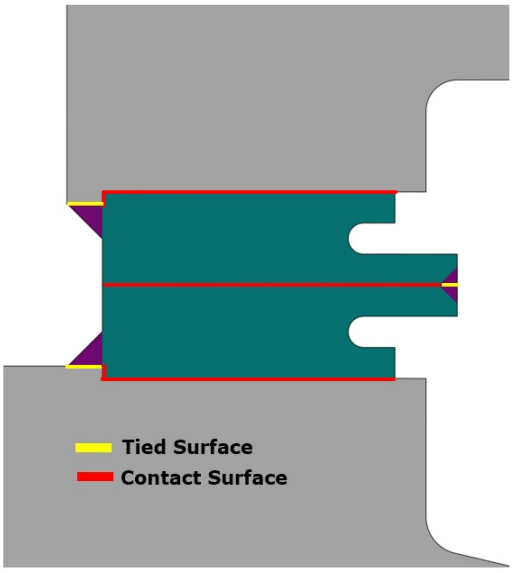

Figure 7. Contact and Tied Surfaces in the FEA Model with the Original (Flat-Lip) Weld Ring Gaskets.

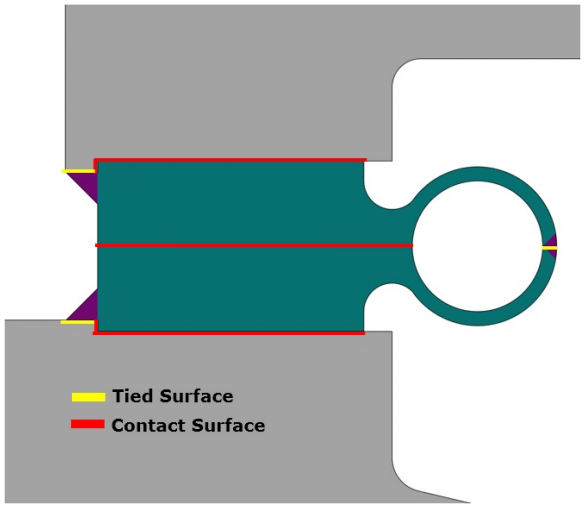

Figure 8. Contact and Tied Surfaces in the FEA Model with Modified Hollow-Lip (Omega) Weld Ring Gaskets.

In addition to the bolted joint joining the flanged extension of the tubesheet and the shell-side of the heat exchanger, the diaphragm seal between the channel shell and the flat channel cover is evaluated using axisymmetric FEA. Figure 9 shows the FEA model of the channel shell-to-channel cover bolted joint (with mesh refinement shown). Similar to the aforementioned FEA models, this model incorporates the bolts using equivalent plane stress elements to facilitate application of the total bolt load. Furthermore, contact is defined between the diaphragm seal and the channel flange with the seal weld tied to the flange face as shown in Figure 10.

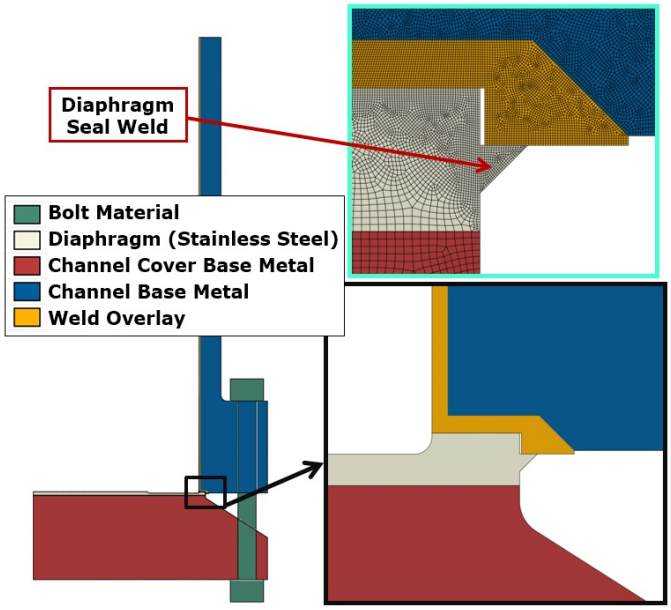

Figure 9. Axisymmetric FEA Model of the Channel Shell-to-Channel Cover Flanged Joint with the Original Diaphragm Seal Design.

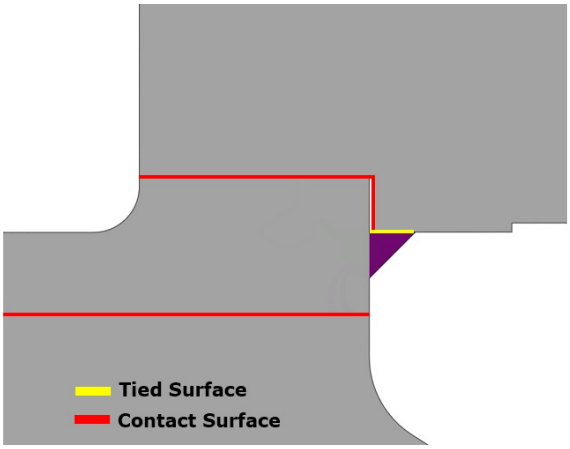

Figure 10. Contact and Tied Surfaces in the FEA Model with the Original Diaphragm Seal Design.

The computational analyses summarized herein provide a means to better understand the root-cause of the cracking (and subsequent through-wall leak) in the seal weld of the original flat-lip weld ring gasket configuration. Additionally, in this

study, comparisons are made using these FEA models to evaluate the diaphragm seal and potential design improvements, including the effects of changing the following:

- Geometry of the weld rings (flat-lip vs. hollow-lip designs)
- Assumed friction coefficient on contact surfaces
- Amount of applied bolt preload
- Inclusion of flexible graphite insert on weld ring gaskets
- Modifying diaphragm gasket material
- Size of the diaphragm gasket seal weld

ORIGINAL WELD RING GASKET ANALYSIS RESULTS

Steady-state heat transfer analysis is carried out on the axisymmetric FEA models to mimic typical metal temperature gradients during operation. Internal shell-side and tube-side pressure is applied to the model along with steady state temperatures following an initial preload step in the analysis where only bolt load is applied (at ambient temperatures) to simulate the flanged joint assembly process. In the ensuing analysis steps where other loads are applied to the model, the bolt preload is held constant to realistically simulate the restraint of the bolts. Figure 11 shows contours of equivalent operating temperature (in °F) for the shell-side-to-flanged extension of the tubesheet joint. These metal temperature distributions are calculated by assigning heat transfer coefficients to all surfaces in the FEA model and specifying the appropriate sink temperatures based on process data. It is noted that an equivalent heat transfer coefficient is applied to the tube-side face of the tubesheet to attempt to account for flow through the perforations in the tubesheet itself.

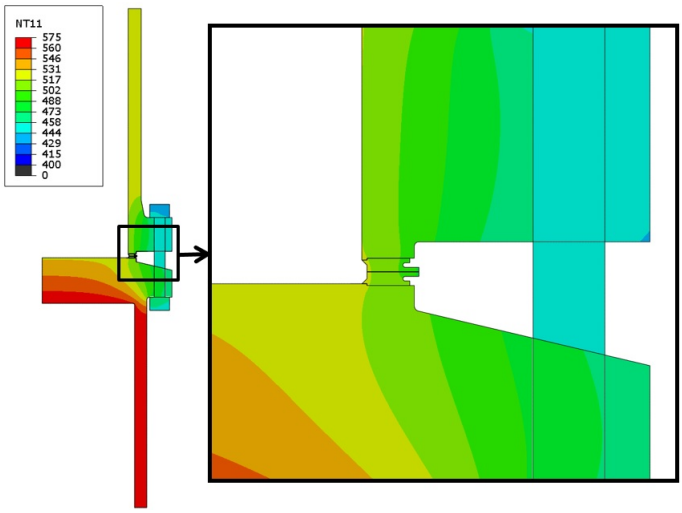

Figure 11. Steady-State Temperature Distributions (°F) in the Original Weld Ring Gasket FEA Model.

Figure 12 shows contours of deflections (in inches) and equivalent elastic von Mises stress (in psi) in the shell-side-to-tube-side flanged connection for bolt loading only and for steady state operating loads (including bolt load, pressure, and temperature). In this figure, the applied deformation scale factor is 50. With exaggerated deflection plotted, the rotation of the flanges is evident, as is the propensity for differential radial movement between the two weld ring gaskets. This effect is even more evident in Figure 13, which shows a close-up view of the weld ring gasket deflections under bolt loads only (no metal temperature gradients present in the model). This figure shows overall deflections in the flat-lip weld ring gaskets with the seal weld modeled and contours of radial deflections (in inches) with the seal weld removed to show the propensity for differential radial movement under bolt loading (the deformation scale factor for both images in Figure 13 is set to 25).

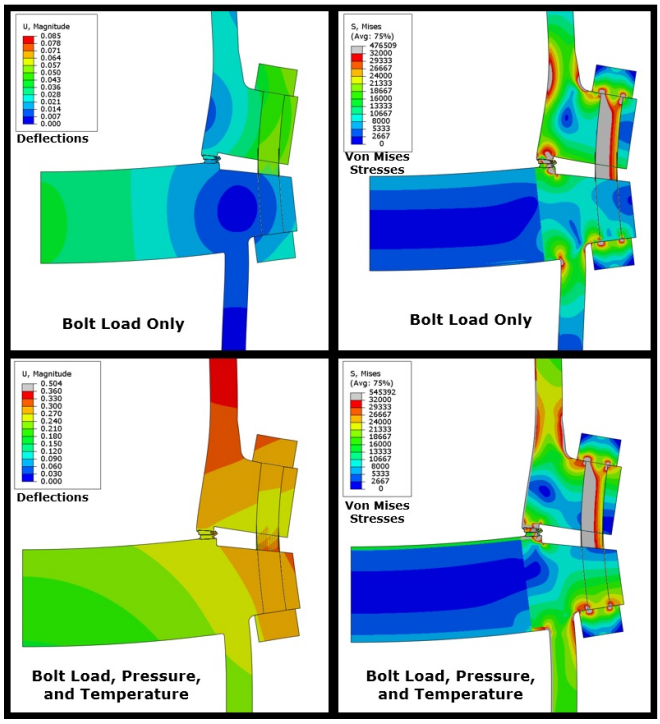

Figure 12. Deflections (in inches) and von Mises Stress (in psi) for Bolt Loading and Operating Loads (Deformation Scale Factor = 50).

The differential movement of the weld ring gaskets in Figure 13 is likely an artifact of the tube-side tapered flange exhibiting more compliance than the shell-side flange, and thus, rotating more during bolt-up. This overall difference in flange rotation results in a bending behavior of the weld ring gaskets as shown; this effect also induces significant shear stresses in the outer flat-lip seal weld and the top (shell-side) weld ring gasket attachment fillet weld on the inside diameter of the weld ring.

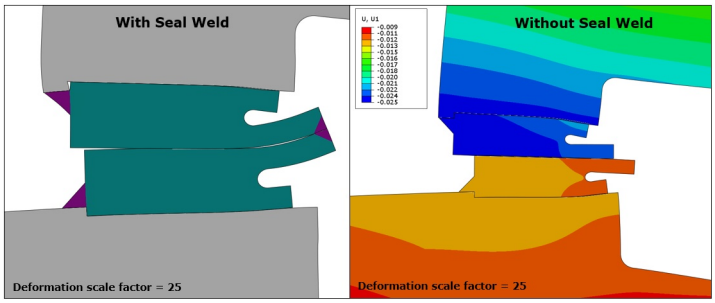

Figure 13. Deflections with the Seal Weld Modeled and Contours of Radial Deflections (inches) with Seal Weld Removed for Bolt Load.

The phenomenon of differential radial movement (and subsequent shear stresses in the seal weld) is exacerbated by operating temperature gradients in the shell-side and tube-side flanges; however, bolt load is the dominant factor in generating bending and shear stresses in the seal weld. Figure 14 shows a close-up view of equivalent elastic (von Mises) stress contours in the flat-lip weld ring gaskets, and in particular, in the seal weld under bolt load and operating pressures and temperatures (the outline of the seal weld is drawn in this figure). Elastic stresses indicate that yielding through the thickness of the outer seal weld would be likely. This is confirmed via elastic-plastic FEA simulations.

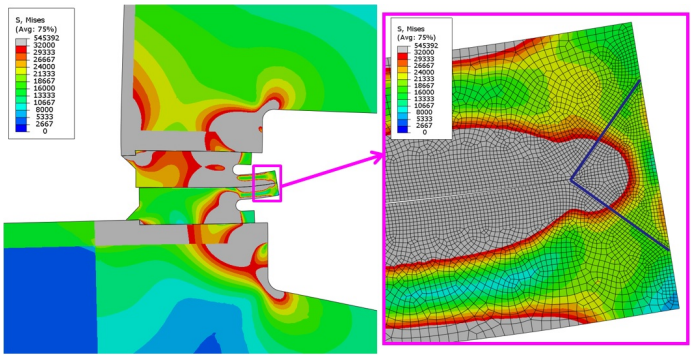

Figure 14. Contours of Elastic von Mises Stress (psi) in the Flat-Lip Weld Ring Gaskets and Seal Weld Under Operating Loads.

The following FEA simulations (load cases) are carried out to compare the overall effects of bolt preload, internal shell-side and tube-side pressure, and steady-state operating temperatures:

- Nominal bolt load only
- Nominal bolt load and pressure
- Nominal bolt load, pressure, and temperature
- 70% of nominal bolt load, pressure and temperature
- Bolt load of 75% yield stress, pressure, and temperature

A comparison of calculated elastic shear stress through the flat-lip seal weld is given in Figure 15 for the aforementioned load cases. This figure shows shear stresses through the thickness of the idealized weld deposit (moving from the root of the weld to the outside surface of the gasket lips). It can be seen that local stresses in the seal weld significantly exceed the yield strength of the gasket material, such that local plasticity would certainly be anticipated in and around the seal weld deposit. Additionally, this figure highlights the overall effect of adjusting the bolt load; that is, adding internal pressure and changing temperature has a relatively minimal effect on predicted shear stress compared to the magnitude of bolt load applied during assembly.

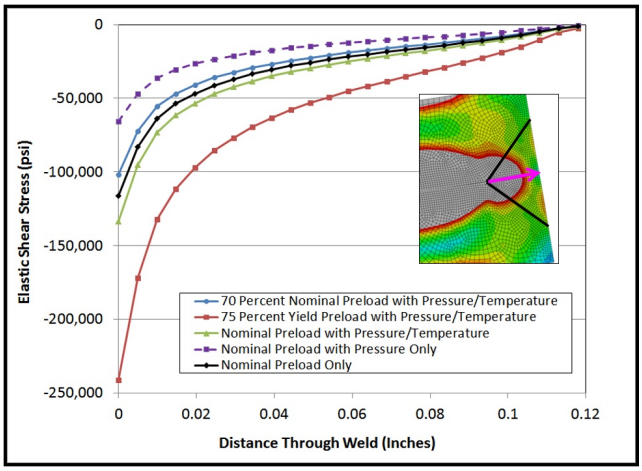

Figure 15. Through-Thickness Elastic Shear Stress in the Flat-Lip Weld Ring Gasket Seal Weld For Different Load Cases.

Linearized elastic membrane shear stresses through the lip seal weld and top inside fillet (attachment) weld also significantly exceed ASME Section VIII Division 1 [4] allowable shear stress thresholds for both groove and fillet welds (as specified in Paragraph UW-15). Allowable shear stresses for groove and fillet welds are specified as 60% and 49% of Code-based allowable stress, respectively [4]. In fact, calculated elastic membrane (average) stress values in the attachment and seal welds are multiples of these allowable values for the flat-lip design. Additionally, in order to evaluate the overall sealing capacity of the above mentioned load cases, contact pressure (in psi) across the face of the weld ring gasket interface is plotted in Figure 16. Compression in a portion of the weld rings is maintained in all cases.

Lastly, in order to quantify the effects of the assumed friction coefficient assigned to contact surfaces in the FEA, simulations with varying friction coefficients are carried out. Figure 17 shows elastic von Mises stress through the thickness of the lip seal weld for no friction coefficient and assumed friction coefficients of 0.1, 0.2, and 0.3. This figure shows that the effects

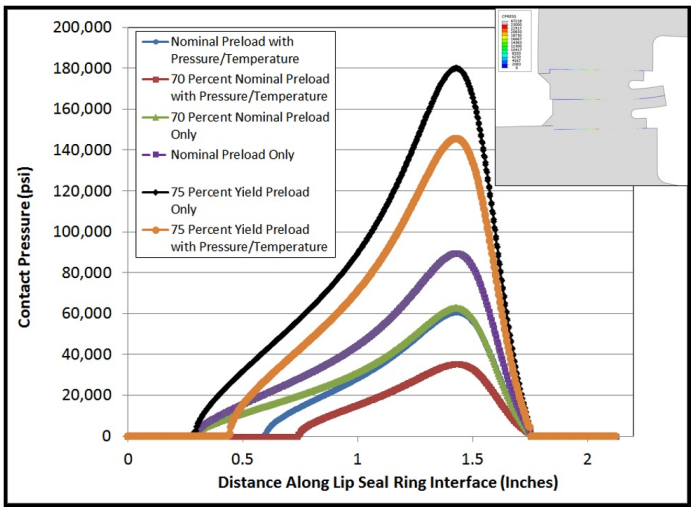

Figure 16. Contact Pressure (psi) Across the Face of the Weld Ring Gasket Interface For Different Load Cases.

of friction reduce stresses at the seal and fillet weld locations, but these stresses are still beyond the Code specified shear allowable values discussed above, regardless of assumed friction coefficient. In reality, the actual friction coefficient is hard to predict and is likely sensitive to surface roughness and cleanliness, etc. The reduction in weld shear stress from increased friction is expected, but given the unknowns in surface conditions, a lower friction coefficient should be considered for conservatism (hence the reason the computational comparisons discussed herein assume no friction between gaskets or between gaskets and their respective flange faces).

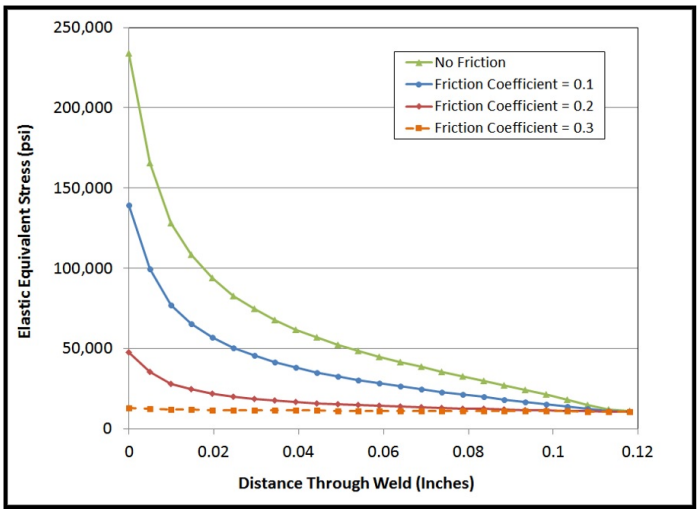

Figure 17. von Mises Stress (psi) Through the Flat-Lip Seal Weld for Varying Friction Coefficients.

ALTERNATIVE GASKET DESIGN ANALYSIS RESULTS

Given the high shear stresses predicted in the flat-lip weld ring gasket seal weld under bolt load and typical operating loads, an alternative hollow-lip (Omega) seal configuration (see Figure 8) is investigated using the same FEA model and loading conditions. Figure 18 shows the deformed shape in the weld rings due to bolt load for the original (flat-lip) and alternative (hollow-lip) designs (with a deformation scale factor of 25). This figure shows how the Omega seal design flexes and distorts to better accommodate differential radial movement in adjoining weld rings relative to the original design.

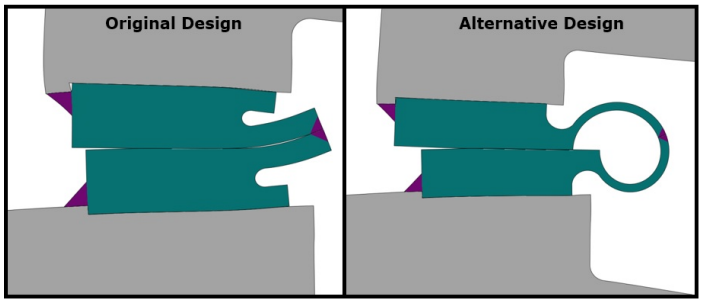

Figure 18. Deflections Due to Bolt Load for Original (Flat-Lip) and Alternative (Hollow-Lip) Designs (Deformation Scale Factor = 25).

To better demonstrate the effect of this added compliance in the lips of the gaskets, Figure 19 shows contours of elastic stress in the seal weld region of the original and alternative designs due to bolt load, pressure, and temperature loading. This figure clearly shows a significant reduction in equivalent stress near the seal weld region of the hollow-lip configuration relative to the flat-lip design. Furthermore, Figure 20 plots equivalent elastic stress through the thickness of the seal weld for both designs for different load cases. The notable reduction in equivalent and shear stress in the outer seal weld can be quantified by comparing stress distributions directly in this figure. It is noted that one comparison in Figure 20 considers the inside of the hollow-lips to be pressurized to full operating pressure (this simulates the scenario of separation between the faces of the weld rings).

While stresses in the outer lip seal weld are significantly reduced for this alternative weld ring design, elevated shear stresses on the inside attachment fillet weld are still observed (above Code-based allowables). In an effort to improve the alternative design further, an optimized hollow-lip design is evaluated using FEA. Figure 21 shows this optimized design, where the attachment fillet weld is moved from the inside surface of the weld ring gaskets to the outside surface and a flexible graphite ring (insert) is added to a portion of the weld ring gasket surfaces.

Figure 22 shows a comparison of contours of elastic shear stress in the original weld ring gasket design versus the optimized

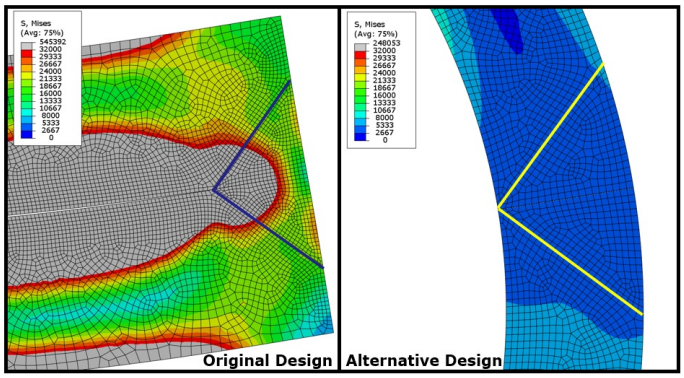

Figure 19. Contours of Elastic von Mises Stress (psi) in the Original and Alternative Design Seal Welds Under Operating Loads.

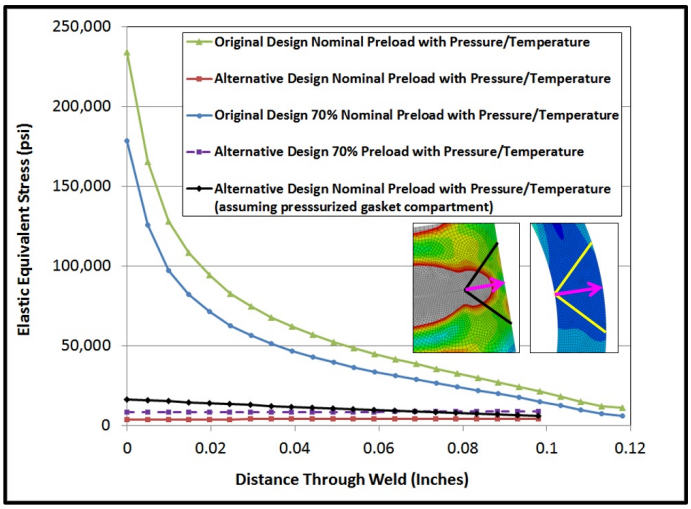

Figure 20. Elastic von Mises Stress (psi) Through the Original and Alternative Design Seal Welds For Different Load Cases.

hollow-lip design with a flexible graphite insert and attachment welds moved to the outside surface (the deformation scale factor is 10). The loading in this figure includes bolt load, shell-side and tube-side internal pressure, and steady-state operating temperatures. Shear stresses predicted in both the seal and attachment welds are significantly reduced in this optimized hollow-lip design relative to the original flat-lip configuration. Sufficient compression is maintained across the flexible graphite layer in the optimized gasket design to maintain adequate sealing as well as shown in Figure 23. This figure shows contours of longitudinal stress (in psi) for the optimized weld ring gasket design for bolt load only and for bolt load plus operating pressure and temperature. Any tensile stresses are identified by the gray contours in this figure (all other contour colors represent compressive stress).

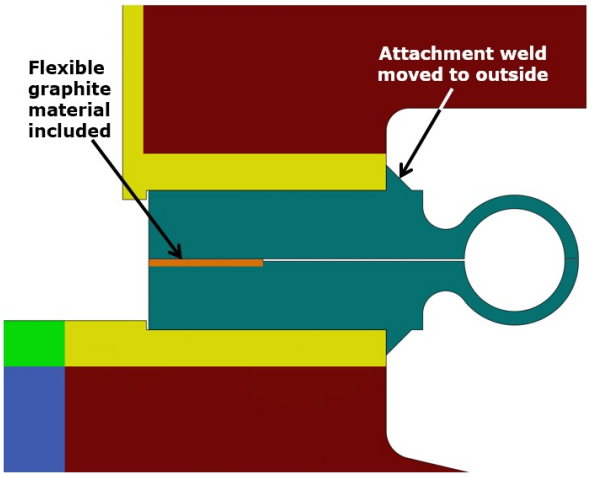

Figure 21. Optimized Weld Ring Gasket Design with Graphite Material and Relocated Attachment Weld.

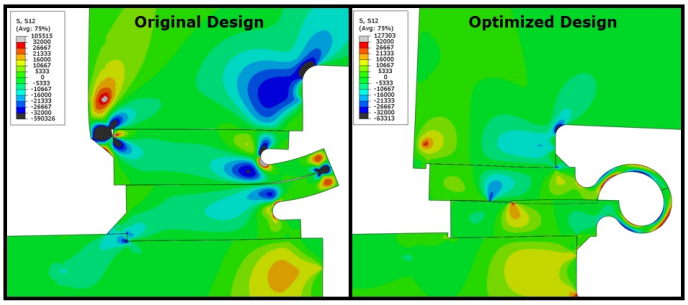

Figure 22. Contours of Elastic Shears Stress (psi) in the Original and Optimized Gasket Designs (Deformation Scale Factor = 10).

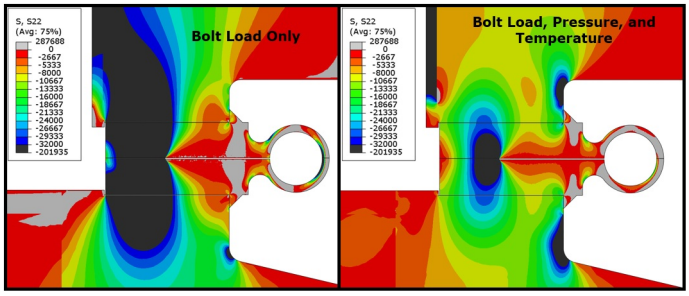

Figure 23. Contours of Elastic Longitudinal (Compressive) Stress (psi) in the Optimized Gasket Design for Bolt and Operating Loads.

DIAPHRAGM SEAL ANALYSIS RESULTS

Once again, axisymmetric FEA is employed to evaluate the thermal-mechanical behavior of the flat channel cover diaphragm seal. Contours of steady-state metal temperature distributions (in °F) based on heat transfer analysis are shown in Figure 24.

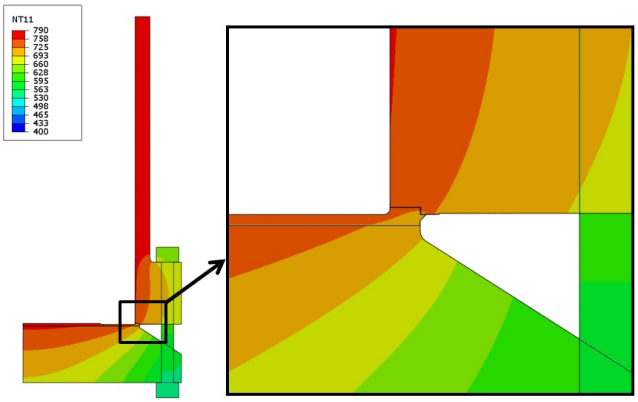

Figure 24. Steady-State Temperature Distributions (°F) in the Original Channel Cover Diaphragm Seal FEA Model.

This diaphragm seal design did not leak or fail in service, but the following design modifications are nevertheless investigated for this bolted joint assembly.

- Doubling the size of the outer seal weld
- Changing the diaphragm material to Inconel

In particular, the stresses in the outer seal weld and the ability to maintain sufficient compression to guarantee leak free operation at the diaphragm-to-flange interface throughout operation are of importance. To compare the overall behavior under load, Figure 25 shows model deflections under bolt preload and operating loads (including internal tube-side pressure and temperature). In this figure, the deformation scale factor is 100. Furthermore, the overall behavior during bolt-up includes some separation between the diaphragm gasket and the flat channel cover due to bending behavior in the diaphragm seal gasket. This separation is eliminated once internal pressure is applied.

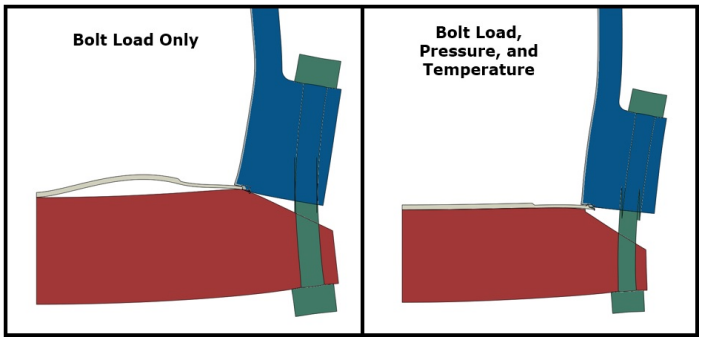

Figure 25. Deflections in the Original Channel Cover Diaphragm Seal Assembly Due to Preload and Operating Loads (Deformation Scale Factor = 100).

Figure 26 shows the longitudinal (compressive) stress distributions in the diaphragm seal at the interface with the channel flange face. In this figure, compressive stress due to operating loads is compared for nominal bolt load, 70% nominal bolt load, and 50% nominal bolt load. It can be observed that adequate compression (sealing capability) is generally demonstrated for all three of these load cases.

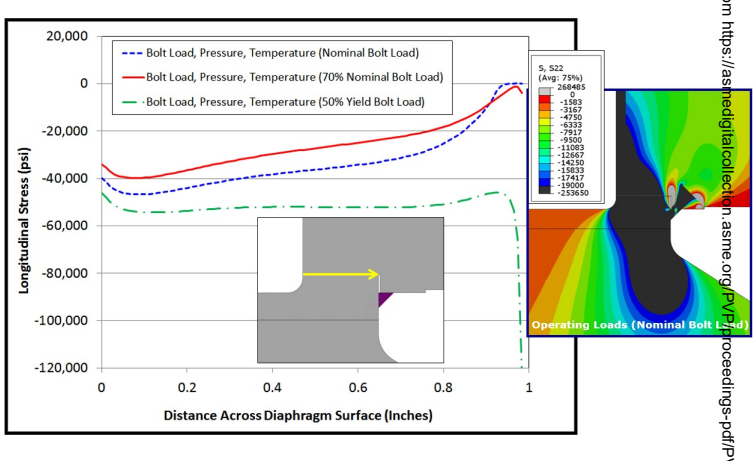

Figure 26. Compressive Stress (psi) in the Diaphragm Gasket for Varying Amounts of Bolt Load.

The behavior of this assembly, with operating temperature gradients applied, shows high radial elastic stresses in the outer seal weld (exceeding Code allowables). This behavior is largely due to the coefficient of thermal expansion mismatch between the stainless steel diaphragm gasket and the low-chrome base metal of the channel cover and flanges (where the diaphragm gasket expands more than the tube-side base metal and is put into compression due to restrained thermal expansion). In an effort to potentially mitigate this effect, a simulation with an Inconel diaphragm is carried out. Figure 27 compares radial stresses in the FEA for bolt load, internal pressure, and temperature for the models with the original stainless steel diaphragm and an alternative Inconel diaphragm.

Figure 27 shows that changing to an Inconel diaphragm notably reduces radial stresses in the outer seal weld. This outcome is expected since the coefficient of thermal expansion of Inconel more closely matches that of the tube-side base metal, thus minimizing restrained thermal expansion effects. A second alternative design incorporates both the Inconel diaphragm and an outer seal weld equal to double the size of the original weld. Figure 28 compares radial stress radial stresses in the model for bolt load, internal pressure, and temperature for the configurations with the original stainless steel diaphragm and an alternative (optimized) Inconel diaphragm with a larger outside seal weld.

Linearized shear membrane (average) stresses through the diaphragm seal fillet weld are compared (bolt load, pressure, and

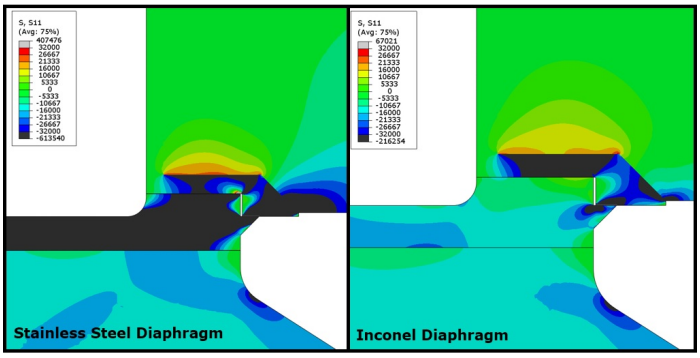

Figure 27. Contours of Radial Stresses (psi) in the Diaphragm Seal Assembly with Stainless Steel and Inconel Diaphragms.

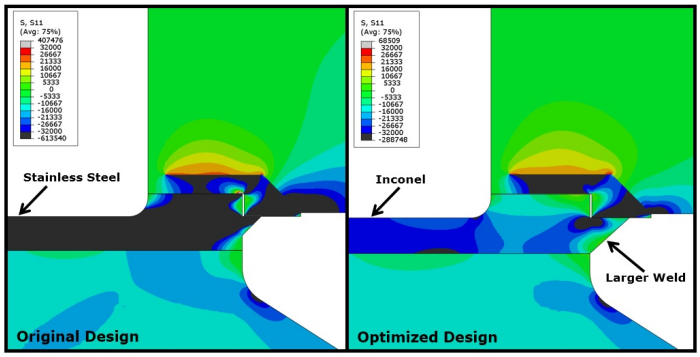

Figure 28. Contours of Radial Stresses (psi) in the Diaphragm Seal Assembly for the Original and Optimized Designs.

temperature) for the simulation with the original seal weld and the optimized design (assuming no friction). FEA results indicate that increasing the size of the seal weld is beneficial in significantly reducing shear stresses in the seal weld, and changing the diaphragm to Inconel reduces stresses further, making this optimized design preferable relative to the original configuration. These normalized membrane shear stress comparisons in the seal weld for the original and optimized diaphragm seal designs are given in Figure 29 for bolt load and operating pressure and temperature. This figure shows the two stress classification line (SCL) locations in the seal weld where stress linearization is performed in each FEA model (see Reference [34] for more information on stress classification). The significant reduction in seal weld shear stresses for the optimized design (highlighted in Figure 29) directionally reduces the likelihood of initiating or propagating a crack in the weld deposit region and mitigates the chances of experiencing an in-service leak. Even though this optimized design exhibits better overall sealing characteristics relative to the original configuration, the presence of an initial weld defect could detrimentally influence the overall damage tolerance.

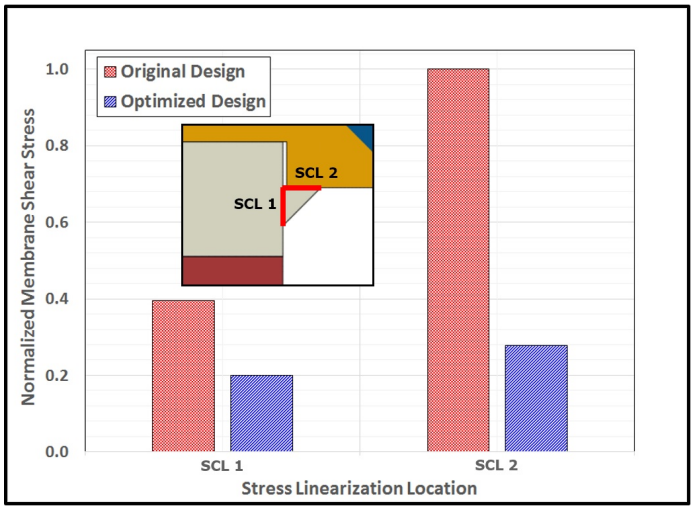

Figure 29. Comparison of Normalized Membrane (Average) Shear Stress in the Diaphragm Seal Weld for the Original and Optimized Designs.

SUMMARY AND CONCLUSIONS

In this paper, case studies of several different weld ring gasket designs and diaphragm seal configurations are evaluated using thermal-mechanical FEA for bolted joints on a high-pressure heat exchanger. Bolt loads, internal pressure, and steady-state operating temperatures are evaluated and gasket behavior is simulated using contact surfaces. The comparisons presented herein offer meaningful design guidance that can be leveraged by equipment designers, fabricators, and owner-users to better determine the most damage tolerant weld ring gasket and diaphragm seal designs. Even today, new designs of these bolted joints are often deficient or less than ideal for their given application and are therefore prone to leakage and premature failure. Furthermore, establishing and implementing the optimal weld ring gasket and diaphragm seal designs upfront will minimize equipment downtime in the future and improve overall bolted joint reliability.

The initial analysis performed was intended to evaluate the root cause of a through-wall crack and subsequent leak in the original flat-lip weld ring gasket between the shell-side and tube-side flanges. This analysis revealed that the lack of ability of the original, flat-lip gasket to accommodate differential flange rotation and radial thermal growth, in addition to the potential for an inherent flaw (single-sided weld) associated with the weld ring geometry, is problematic from a design standpoint. To this end, ensuring quality attachment and seal welds (and performing proper inspection to mitigate gasket misalignment and weld defects) during fabrication and assembly represents an essential aspect of achieving long-term reliability. Furthermore, the effects of lip seal misalignment, weld defects, and operational upset scenarios were not explicitly considered in this study, but these anomalies could substantially increase the likelihood of in-

service leakage or failure.

Elastic stresses through the flat-lip seal weld indicate that shear failure and crack initiation at the root of the seal weld would be likely. Furthermore, elastic stresses at both the lip seal weld and the inside attachment fillet weld significantly exceed ASME Code allowable shear stress limits. Results indicate that bolt load (and subsequent flange and gasket rotation), not internal pressure or metal temperature gradients, is the dominant contributor to over-stress conditions in the seal and attachment welds. Additionally, sensitivity to specified bolt load and assumed friction coefficient is also quantified herein. Increasing the friction coefficient generally reduces predicted stresses in the gasket and diaphragm attachment and seal welds, but establishing an accurate friction coefficient is difficult due to unknowns in gasket and flange face surface conditions.

In light of the original analysis results, several design modifications are investigated to attempt to improve damage tolerance and long-term reliability of this gasketed joint. Changing the weld ring gaskets from a flat-lip to a hollow-lip (Omega) design significantly reduces shear stresses in the outside seal weld due to the added flexibility associated with the rounded lip design. Furthermore, in general, hollow-lip weld ring gasket designs can inherently better accommodate differential radial movement due to thermal-mechanical loading compared to flat-lip configurations. After evaluating several different variants of hollow-lip designs, a layout with the attachment fillet weld located on the outside of the flanges with a flexible graphite insert over a portion of the gasket face proves to be the most damage tolerant design (lowest shear stresses in the welds) with the best overall sealing characteristics.

Additionally, thermal-mechanical FEA is carried out on the flat channel cover-to-channel shell diaphragm seal assembly. While the overall sealing ability of this joint proves to be sufficient for different magnitudes of bolt load, shear stresses in the outer seal weld are elevated under typical operating loads (mainly due to differential thermal expansion of the diaphragm gasket relative to the channel base metal). Since there is no inherent flexibility at this joint to accommodate differential radial thermal expansion, changing the diaphragm material from stainless steel to Inconel reduces stresses in the seal weld (coefficient of thermal expansion mismatch is minimized). Furthermore, doubling the size of the outer seal weld reduces membrane (average) shear stresses in the weld deposit even more and highlights a design with the best likelihood of long-term reliability and leak-free operation. Lastly, FEA studies, such as the one described in this paper, offer valuable insight into the thermal-mechanical behavior of complex bolted joint assemblies and provide the analytical means to optimize gasket designs and bolting parameters.

REFERENCES

[1] Kempchen, 2014. *Kempchen Weld Ring Gasket Brochure*. Kempchen Dichtungstechnik GmbH, Oberhausen, Germany.

[2] Singh, K., and Soler, A., 1984. *Mechanical Design of Heat Exchangers and Pressure Vessel Components*. Arcturus Publishers, Inc., Cherry Hill, NJ.

[3] TEMA, 2007. *Standards of the Tubular Exchanger Manufacturers Association*, 9 ed. Tarrytown, NY.

[4] ASME, 2006 Addenda. *Section VIII Division 1: Rules for Construction of Pressure Vessels*. American Society of Mechanical Engineers Boiler and Pressure Vessel Committee, New York, NY.

[5] Hughes, D., Cesarini, J., and Howard, E., 2007. "Success in a High-Pressure Refinery Heat Exchanger Diaphragm Removal/Retrofit". *Maintenance Technology*, Nov.

[6] McGuffie, S., Porter, M., and Martens, D., 2010. "Diaphragm Closure Analysis Using Nonlinear FEA and CFD". In ASME Pressure Vessels and Piping Conference. PVP2010-25833.

[7] Martens, D., and Porter, M., 1994. "Investigation and Repair of Heat Exchanger Flange Leak". *ASME Developments in Pressure Vessels and Piping,* **278**.

[8] Porter, M., and Martens, D., 2006. "Reinvestigation of a Heat Exchanger Flange Leak". In ASME Pressure Vessels and Piping Conference. PVP2006-ICPVT-11-93731.

[9] Sato, T., and Kado, K., 2005. "Inelastic Analysis of Dissimilar Material Flanges With Metal Ring Gaskets at Elevated Temperature". In ASME Pressure Vessels and Piping Conference. PVP2005-71131.

[10] Prueter, P., Dewees, D., Macejko, B., and Brown, R., 2013. "Assessing Flanged Joint Leakage and Tube-to-Tubesheet Joint Failure Due to Fluid Temperature Differentials in a Floating Head Heat Exchanger using Finite Element Analysis". In ASME Pressure Vessels and Piping Conference. PVP2013-97576.

[11] Dudley, W., 1961. "Deflection of Heat Exchanger Flanged Joints as Affected by Barrelling and Warping". *Transaction of ASME Series B,* **83**, pp. 460–466.

[12] Kerkhof, W., 1951. "New Stress Calculations and Temperature Curves for Integral Flanges". *Proceedings of the 3rd World Petroleum Congress,* **8**, pp. 146–168.

[13] Bickford, J., Hayashi, K., Chang, A., and Winter, J., 1989. *Welding Research Council Bulletin 341: A Preliminary Evaluation of the Elevated Temperature Behavior of a Bolted Flanged Connection*. Welding Research Council, Inc., New York, NY.

[14] Brown, W., and Brodzinski, R., 2005. "Case Study of Temperature Analysis Performed on a 45 inch Diameter Heat Exchanger Flange". In ASME Pressure Vessels and Piping Conference. PVP2005-71340.

[15] Bouzid, A., and Nechache, A., 2005. "Thermally Induced Deflections in Bolted Flanged Connections". *Journal of Pressure Vessel Technology,* **127**, Nov., pp. 394–401.

[16] Bouzid, A., and Nechache, A., 2005. "An Analytical Solution for Evaluating Gasket Stress Change in Bolted

Flange Connections Subjected to High Temperature Loading". *Journal of Pressure Vessel Technology,* **127**, Nov., pp. 414–422.

[17] Nagata, S., and Sawa, T., 2008. "Effects of Temperature Change on Bolt Load and Gasket Load of Bolted Flange Connection With Ring Type Joint Gasket". In ASME Pressure Vessels and Piping Conference. PVP2008-61418.

[18] Kummari, S., Dewees, D., and Brown, R., 2012. "Finite Element Based Analysis of Bolted Joints Under Extreme Loading Conditions". In ASME Pressure Vessels and Piping Conference. PVP2012-78541.

[19] Abid, M., and Ullah, B., 2007. "Three-Dimensional Nonlinear Finite-Element Analysis of Gasketed Flange Joint under Combined Internal Pressure and Variable Temperatures". *Journal of Engineering Mechanics,* **133**, Feb., pp. 222–229.

[20] Al-Sannaa, M., and Alghamdi, A., 2002. "Two Dimensional Finite Element Analysis for Large Diameter Steel Flanges". *Proceedings of the 6th Saudi Engineering Conference,* **5**, Dec., pp. 397–408.

[21] Sato, T., and Kado, K., 2005. "Inelastic Analysis of Dissimilar Material Flanges with Metal Ring Gaskets at Elevated Temperature". In ASME Pressure Vessels and Piping Conference. PVP2005-71131.

[22] Bouzid, A. H., and Galai, H., 2011. "Contact Stress Evaluation of Nonlinear Gaskets Using Dual Kriging Interpolation". *Journal of Pressure Vessel Technology,* **133**(2), Feb.

[23] Bouzid, A. H., and Champilaud, H., 2004. "Contact Stress Evaluation of Nonlinear Gaskets Using Dual Kriging Interpolation". *Journal of Pressure Vessel Technology,* **126**(4), Dec., pp. 445–450.

[24] Krishna, M., Shunmugam, M., and Siva-Prasad, N., 2007. "A Study on the Sealing Performance of Bolted Flange Joints with Gaskets Using Finite Element Analysis". *International Journal of Pressure Vessels and Piping,* **84**(6), June, pp. 349–357.

[25] Mathan, G., and Siva-Prasad, N., 2011. "Studies on Gasketed Flange Joints Under Bending with Anisotropic Hill Plasticity Model for Gasket". *International Journal of Pressure Vessels and Piping,* **88**(11), Dec., pp. 495–500.

[26] Ma, K., Zhang, Y., and Zhang, L., 2014. "Behavior of Bolted Joints with Metal-to-Metal Contact Type Gaskets Under Bolt-Up and Loading Conditions". *Journal of Process mechanical Engineering - Institution of Mechanical Engineers*, Sept.

[27] Brown, W., Derenne, M., and Bouzid, A., 2000. "Determination of the Steady State Operating Temperatures of Pressure Vessel Flange Components: Part 1 - Analytical Methods". *Proceedings of the Pressure Vessels and Piping Conference,* **405**, pp. 95–104.

[28] Brown, W., Derenne, M., and Bouzid, A., 2000. "Determination of the Steady State Operating Temperatures of Pressure Vessel Flange Components: Part 2 - Simplified Methods". *Proceedings of the Pressure Vessels and Piping Conference,* **405**, pp. 105–113.

[29] Brown, W., and Reeves, D., 2001. "Failure of Heat Exchanger Gaskets Due to Differential Radial Expansion of the Mating Flanges". *Proceedings of the Pressure Vessels and Piping Conference,* **416**, pp. 119–122.

[30] Brown, W., Derenne, M., and Bouzid, A., 2001. "Determination of Gasket Stress Levels During High Temperature Flange Operation". *Proceedings of the Pressure Vessels and Piping Conference,* **416**, pp. 185–192.

[31] Brown, W., Derenne, M., and Bouzid, A., 2002. "Determination of Gasket Stress Levels During Thermal Transients". *Proceedings of the Pressure Vessels and Piping Conference,* **433**, pp. 21–28.

[32] Brown, W., 2006. *Welding Research Council Bulletin 510: Analysis of the Effects of Temperature on Bolted Joints*. Welding Research Council, Inc., New York, NY.

[33] Luyt, P., Theron, N., and Pietra, F., 2017. "Non-Linear Finite Element Modeling and Analysis of the effect of Gasket Creep-Relaxation on Circular Bolted Flange Connections". *International Journal of Pressure Vessels and Piping,* **150**(1), Feb., pp. 52–61.

[34] Kroenke, W., 1974. "Classification of Finite Element Stresses According to ASME Section III Stress Categories". In ASME Pressure Vessels and Piping Conference. Pressure Vessels and Piping: Analysis and Computers.